ES Energy & Environment
DOI: https://dx.doi.org/10.30919/esee8c476

Theoretical, Monte Carlo Simulations and Quantitative Structure Activity Relationship Studies on Some Triazole Derivatives as Corrosion Inhibitors for Mild Steel in 1 M HCl

Ramzi. T. T. Jalgham*

Abstract

A possible equation between experimental inhibition efficiencies (IE_{exp}) of corrosion inhibitors and some quantum parameters was sought for some tiazole derivatives in 1 M HCl. Highest occupied molecular energy level (E_{HOMO}), lowest unoccupied molecular energy level (E_{LUMO}), dipole moment (μ), adsorption energy (E_{ads}), energy gap ΔE, surface area (SA) of the molecule, Log of the partition coefficient (*AlogP*) were correlated to corrosion inhibition efficiency. The results showed that a good agreement was found between IE_{exp} and calculated inhibition efficiencies (IE_{calc}) where the correlation coefficients (R^2 and R) between IE_{exp} and IE_{calc} ranged from 0.857 to 0.967 and 0.926 and 0.974, respectively.

Keywords: Triazole derivatives; Modelling studies; Semiempirical Methods-QSAR; Monte Carlo Simulation.
Received: 25 March 2021; Revised: 23 May 2021; Accepted: 27 May 2021.
Article type: Research article.

1. Introduction

Pipelines are considered critical equipment which is used for transporting gases and fluids over long distances. During processes such as acid washing, pickling, and etching corrosion issue exists in the oil business at each phase of creation, from the extraction to refining and storage, preceding use, which requires the utilization of corrosion inhibitors.[1] A metal surface treatment includes removing impurities, such as stains, inorganic contaminants, rust, or scale are mostly achieved by acid solutions. The most frequently used acids are hydrochloric acid and sulfuric acid. To reduce the degradation of metals in hostile environments, organic chemical compounds (corrosion inhibitors) are used.[2]

Most pickling inhibitors are toxic compounds. These chemicals have to be replaced with new environmentally friendly inhibitors due to global demands for environmental awareness and new environmental protection regulations. This article concentrates on non-toxic inhibitors such as triazole derivatives as mild steel corrosion inhibitors in hydrochloric acid. Among the different heterocyclic compounds investigated as corrosion inhibitors, triazole derivatives are considered environmentally friendly compounds. Furthermore, they are highly thermally stable compounds, easily synthesizable, operative at low concentrations, and cost-effective. For these reasons, a lot of emphases researchers to investigate new, environmentally friendly, and low-cost corrosion inhibitors. Thus, the electrochemical technique included (electrochemical impedance spectroscopy (EIS), and potentiodynamic polarization) and quantum chemical analysis, which are mostly used to determine the inhibition and adsorption ability.[3-7]

The performance of corrosion inhibitors has been studied by numerous strategies including experimental and theoretical methodologies. For example, experimental methods, electrochemical impedance spectroscopy (EIS), potentiodynamic polarization, and weight reduction technique are the most common methods used to test the inhibition performance. They are costly and tedious. All these difficulties have been defeated by theoretical methods. The atomic structure, explaining the electronic structure and reactivity of corrosion inhibitors are extremely helpful and all of these are done by quantum chemical studies. On the other hand, numerous quantum chemical studies have found successfully between inhibition efficiency and some quantum parameters such as molecular orbital. Recently, quantitative structure-activity relationship (QSAR) regression or classification models used in chemical studies have been a subject of intense interest in many disciplines of chemistry. Several attempts have been done to achieve the appropriate equations to correlate the experimental data with quantum-

Oil & Gas department, Bani Waleed University (BWU), Bani Waleed City, Libya.
**Email:* ramzittj@gmail.com (R. Jalgham)

chemical properties highest occupied molecular energy level (E_{HOMO}), lowest unoccupied molecular energy level (E_{LUMO}), charges on reactive center, and μ.[8-12]

Semiempirical methods (parameterization model 6 (PM6), parameterization model 3 (PM3), Austin Model 1 (AM1), Recife model 1 (RM1), and modified neglect of differential overlap (MNDO)) have been successfully applied on -hydroxyl-1,2-di(pyridine-2-yl) ethanone (pyridoin), 2-hydroxy-1,2-diphenyl ethanone (benzoin) and benzyl in the correlation of experimental and theoretical inhibition efficiencies. Multiple regressions were performed between the experimental inhibition efficiencies (IE_{exp}) of the inhibitors and the calculated quantum chemical parameters which were obtained for PM6, PM3, AM1, RM1, and MNDO Hamiltonians. From the obtained results, it was found that there is a strong relationship between IE_{exp} and calculated inhibition efficiencies (IE_{calc}), and the correlation coefficient R was about 0.913.[13] QSAR was successfully applied to predict inhibition efficiency 2,5-bis(n-thienyl)-1,3,4-thiadiazoles in sulfuric acid. A linear resistance (LR) model was employed to predict inhibition efficiency with a composite index of more than one parameter, that effect inhibition efficiency. The correlation coefficient was about 0.9.[14] EIS measurements were correlated with some theoretical parameters (the molecular weight (*M.wt*), ΔE, ΔN, and the binding energy (*BE*)), and a multiple linear regression approach using the XLSTAT software was utilized to predict *IE*. It was noticed that the introduction of the binding energy to each composite improve the results where R^2 was about 0.998.[15] Genetic function approximation **(**GFA) was employed in QSAR to correlate the inhibition efficiencies and the molecular structure characteristics of the amino acids. Four GFA-derived models were derived. The calculated corrosion efficiencies of these compounds nicely matched the experimental measurements where the correlation coefficient was about 0.97.[16] QSAR modeling study was done on five phenylpropanoids from Alpinia galanga and other related compounds using the Dragon software to model the obtained experimental data and the molecular descriptors. The penalized multiple linear regression was selected to develop a high-dimensional QSAR model. The model obtained with R^2 = 0.927 could be employed to calculate the IE of related organic compounds. [17]

Therefore, quantum chemical calculations using semi-empirical and density functional theory (DFT) methods were performed on twenty triazole derivatives. The chemical formulae, nomenclature, and structure of the triazole derivatives which were used in this study are shown in Table 1 and Fig. 1. These compounds have been studied experimentally to be corrosion inhibition efficient with efficiencies ranging from 73 – 98.5%.[18-28] Thus, the major aim of this paper is to use semi-empirical and DFT methods to calculate molecular descriptors that relate to the observed inhibition efficiencies of these triazole derivatives as well as to develop QSAR model from the calculated descriptors that could predict the observed inhibition efficiencies.

2. Details of calculation methods

The molecular structures of the selected compounds were tested using quantum chemical calculations. All the quantum calculations using three semi-empirical methods and three DFT methods were carried out at Restricted Hartree-Fock (RHF) level and Double Numerical plus d-functions (DND) as a basis set respectively in the Material Studio 5.5 software for Windows. The size of the DND basis is comparable to Gaussian 6-31G* basis sets. All inhibitors structured were fully optimized geometry without any constraints using default program settings.[29]

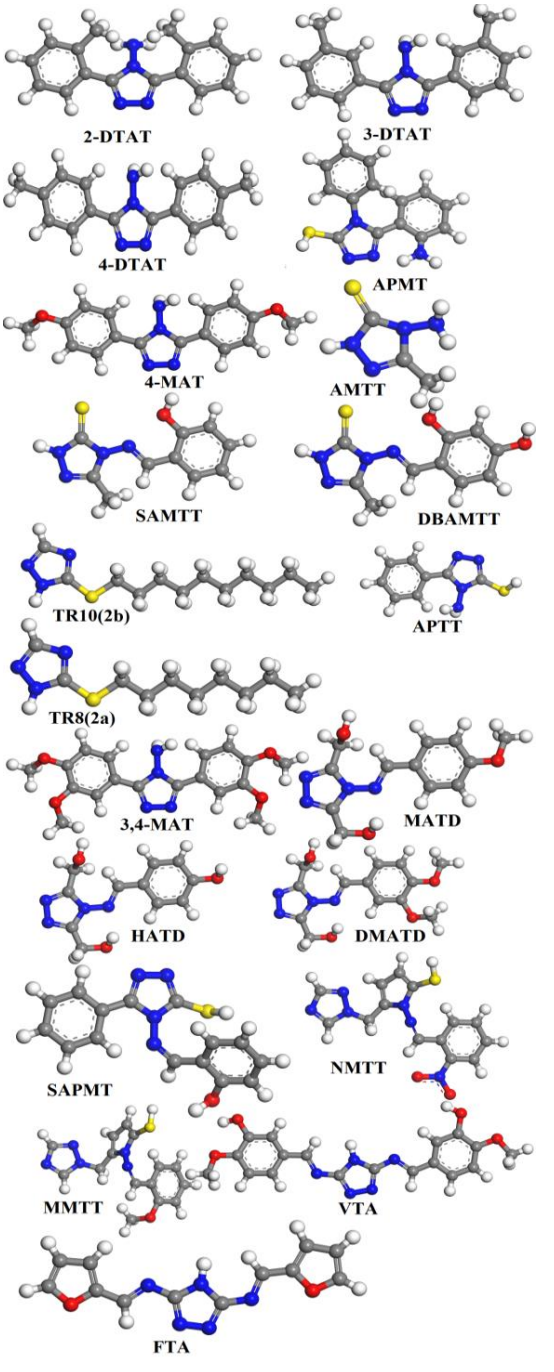

Fig. 1 Chemical structure of triazole derivatives.

Table 1. Names, nomenclature, and molecular properties of studied triazole derivatives.

Full name	Nomenclature	Chemical formula	Net mol. mass	Ref. No
3,5-di(3-tolyl)-4-amino-1,2,4-triazoles	3-DTAT	$C_{16}H_{16}N_4$	264.332	[18]
3,5-di(2-tolyl)-4-amino-1,2,4-triazoles	2-DTAT	$C_{16}H_{16}N_4$	264.332	[18]
3,5-di(4-tolyl)-4-amino-1,2,4-triazoles	4-DTAT	$C_{16}H_{16}N_4$	264.332	[18]
3-aminophenyl-4-phenyl-5-mercapto-1,2,4-triazole	APMT	$C_{14}H_{12}N_4S$	268.338	[19]
3,5-bis(4-methoxyphenyl)-4-amino-1,2,4-triazole	4-MAT	$C_{16}H_{16}N_4O_2$	296.330	[20]
4-amino-5-methyl-4H-1,2,4-triazole-3thiol	AMTT	$C_3H_6N_4S$	130.169	[21]
4-salicylideneamino-3-methyl-1,2,4-triazole-5-thione	SAMTT	$C_{10}H_{10}N_4OS$	234.277	[21]
4-(2,4-dihydroxybenzylideneamino)-3-methyl-1H-1,2,4-triazole-5(4H)-thione	DBAMTT	$C_{10}H_{10}N_4O_2S$	250.276	[21]
5-decylsulfanyl-1,2,4-triazole	TR10(2b)	$C_{12}H_{23}N_3S$	241.397	[22]
5-octylsulfanyl-1,2,4-triazole	TR8(2a)	$C_{10}H_{19}N_3S$	213.343	[22]
4-Amino-5-phenyl-4H-1,2,4-triazole-3-thiol	APTT	$C_8H_8N_4S$	192.240	[23]
3,5-bis(3,4-dimethoxyphenyl)-4-amino-1,2,4-triazole	3,4-MAT	$C_{18}H_{20}N_4O_4$	356.382	[24]
(4-(4-methoxybenzylideneamino)-4H-1,2,4-triazole-3,5-diyl)dimethanol	MATD	$C_{12}H_{14}N_4O_3$	262.269	[25]
(4-(4-hydroxybenzylideneamino)-4H-1,2,4-triazole-3,5-diyl)dimethanol	HATD	$C_{11}H_{12}N_4O_3$	248.242	[25]
(4-(3,4-dimethoxybenzylideneamino)-4H-1,2,4-triazole-3,5-diyl)dimethanol	DMATD	$C_{13}H_{16}N_4O_4$	292.295	[25]
4-salicylideneamino-3-phenyl-5-mercapto-1,2,4-triazole	SAPMT	$C_{15}H_{12}N_4OS$	296.348	[26]
1-(2″-nitrobenzyl)methenylideneamino-2-mercapto-5-(1-(1′,2′,4′-triazol)) methenyl-1,3,4-triazole	NMTT	$C_{14}H_{12}N_6O_2S$	328.350	[27]
1-(2″-methoxybenzyl)methenylideneamino-2-mercapto-5-(1′-(1′,2′,4′-triazol)) methenyl-1,3,4-triazole	MMTT	$C_{15}H_{15}N_5OS$	313.379	[27]
furfuraldine 3,5-diamino-1,2,4-triazole	FTA	$C_{12}H_9N_5O_2$	255.237	[28]
Vanilidine 3,5-diamino-1,2,4-triazole	VTA	$C_{18}H_{17}N_5O_4$	367.365	[28]

Monte Carlo Simulation was utilized to investigate the adsorption behavior of triazole derivatives on Fe (110) plane surface. The adsorption locator module, COMPASS as force field and Ewald technique as summation method for periodic systems employed to perform Monte Carlo simulations in a simulation box (28.66 Å × 22.93 Å × 56.48 Å) with periodic boundary conditions.[30]

SPSS program version 10.0 for Windows was utilized to perform Statistical analyses. The quantum chemical and adsorption energy parameters (E_{HOMO}, E_{LUMO}, μ, ΔE, SA, AlogP, and E_{ads}) were considered to solve the non-linear equations. The method of Levenberg-Marquardt with the unconstrained sum of squared residuals in the SPSS program was employed to perform Non-linear regression to get a higher correlation coefficient.[31] A correlation coefficient means a statistical relationship between two variables (IE_{exp} and IE_{calc}). Many types of correlation coefficients exist, and all will always lie between -1 to 1 where the strongest possible agreement is very close to ±1. The Pearson product-moment correlation coefficient (R^2) measures the strength and direction of the linear relationship. The correlation coefficient (R) is a measure of how well and how close the relationship between two variables (IE_{exp} and IE_{calc}) is.[32]

3. Results and discussion

The experimental inhibition efficiencies (IE_{exp}) of the studied inhibitors were studied by electrochemical impedance spectroscopy (EIS). In this work, QSAR for inhibition of corrosion inhibitors has been done using three semiempirical methods and three DFT methods. Table 2 and Table 3 represent the results of quantum chemical calculations by these methods for compounds in Fig. 1.

The optimized structures (global energy minima) of triazole derivatives using AM1 are shown in Fig. 2. The energy of HOMO and LUMO and their distribution on molecules are very important in defining the reactivity. Most frequently, the capability of the molecule to donate electrons is connected to E_{HOMO} whereas E_{LUMO} is associated with the ability to receive electrons. Therefore, a higher value of E_{HOMO} and a lower value of E_{LUMO} facilitate the adsorption process.[33-38] It can be seen from Table 2 and Table 3 that the calculated values of E_{HOMO} and E_{LUMO} for triazole derivatives are not comparable to the obtained values of IE_{exp} and the obtained quantum chemical parameters changed irregularly with inhibition IE_{exp}.

This proposed that the inhibitors were maybe not one or the other neither the acceptor nor the donor of the electrons. It could be deduced that there was no electron transfer between the active centers of triazole inhibitors and the metal surface.

Table 2. Quantum chemical parameters of triazole derivatives using semiempirical methods.

Method	Compound	E_{HOMO}(eV)	E_{LUMO}(eV)	μ(Debye)	SA(Å^2)
AM1	3-DTAT	-8.966	-0.414	5.779	306.798
	2-DTAT	-9.251	-0.283	5.379	303.578
	4-DTAT	-8.846	-0.443	5.511	307.409
	APMT	-8.547	-0.432	3.672	278.850
	4-MAT	-8.648	-0.388	4.541	324.768
	AMTT	-8.772	-0.129	3.098	143.402
	SAMTT	-8.507	-0.490	5.432	246.833
	DBAMTT	-8.496	-0.516	4.390	258.299
	TR10(2b)	-8.692	-0.035	2.648	323.133
	TR8(2a)	-8.692	-0.036	2.646	279.443
	APTT	-8.605	-0.447	4.423	203.762
	3,4-MAT	-8.727	-0.580	2.113	384.059
	MATD	-9.259	-0.965	7.183	287.893
	HATD	-9.354	-1.019	6.490	267.400
	DMATD	-9.126	-0.984	8.099	319.011
	SAPMT	-8.595	-0.883	3.739	297.219
	NMTT	-9.094	-1.611	7.807	326.670
	MMTT	-8.700	-0.663	6.853	337.046
	FTA	-8.630	-1.321	6.400	278.139
	VTA	-8.502	-1.156	1.420	394.798
PM3	3-DTAT	-9.073	-0.661	6.152	304.217
	2-DTAT	-9.605	-0.244	5.571	305.242
	4-DTAT	-8.965	-0.672	5.712	303.718
	APMT	-8.698	-0.544	4.368	287.422
	4-MAT	-8.783	-0.628	4.867	320.622
	AMTT	-8.772	-0.760	3.953	142.953
	SAMTT	-8.479	-1.064	6.948	244.345
	DBAMTT	-8.425	-1.032	7.988	253.713
	TR10(2b)	-9.079	-0.561	2.351	326.097
	TR8(2a)	-9.079	-0.561	2.349	282.466
	APTT	-8.942	-0.741	4.481	200.522
	3,4-MAT	-8.966	-0.876	6.990	386.125
	MATD	-9.391	-1.259	7.351	287.253
	HATD	-9.448	-1.289	6.976	267.777
	DMATD	-9.312	-1.277	8.025	314.676
	SAPMT	-9.052	-0.982	4.924	307.691
	NMTT	-9.649	-1.531	7.160	332.395
	MMTT	-8.627	-0.660	7.538	337.989
	FTA	-8.809	-1.370	6.090	277.014
	VTA	-8.690	-1.252	2.125	393.078
PM6	3-DTAT	-9.134	-0.588	7.454	307.424
	2-DTAT	-9.459	-0.437	6.790	308.715
	4-DTAT	-8.943	-0.465	6.950	306.839
	APMT	-8.579	-0.641	2.887	281.923
	4-MAT	-8.666	-0.420	5.793	327.543
	AMTT	-8.726	-0.313	3.380	145.176
	SAMTT	-8.493	-0.980	3.902	245.469
	DBAMTT	-8.448	-0.933	3.146	256.165
	TR10(2b)	-9.059	-0.277	1.976	325.739
	TR8(2a)	-9.058	-0.275	2.055	281.811
	APTT	-8.990	-0.686	3.932	206.716
	3,4-MAT	-8.346	-0.577	5.219	383.324
	MATD	-9.270	-1.237	9.090	290.177
	HATD	-9.481	-1.352	8.093	266.943
	DMATD	-8.815	-1.254	10.100	316.358
	SAPMT	-9.072	-1.090	3.703	298.762
	NMTT	-9.291	-2.023	12.014	325.482
	MMTT	-8.629	-1.058	8.645	338.218
	FTA	-9.087	-1.684	6.879	277.037
	VTA	-8.574	-1.283	4.998	392.216

Table 3. Quantum chemical parameters of triazole derivatives using DFT methods.

Method	Compound	E_{HOMO}(eV)	E_{LUMO}(eV)	μ(Debye)	SA(Å^2)
PWC	3-DTAT	-5.244	-2.053	2.326	1071.125
	2-DTAT	-5.274	-1.863	2.261	1020.895
	4-DTAT	-5.143	-1.983	2.137	1067.129
	APMT	-4.718	-2.086	1.385	965.650
	4-MAT	-4.802	-1.773	1.290	1134.745
	AMTT	-5.070	-1.012	0.897	545.855
	SAMTT	-4.910	-2.570	1.655	891.686
	DBAMTT	-4.547	-2.612	3.199	931.932
	TR10(2b)	-5.398	-0.826	1.069	1126.015
	TR8(2a)	-5.403	-0.831	1.055	985.291
	APTT	-5.379	-2.120	1.945	750.651
	3,4-MAT	-4.851	-1.908	1.134	1328.527
	MATD	-5.606	-2.946	3.468	992.973
	HATD	-5.642	-3.006	3.262	930.451
	DMATD	-5.569	-2.931	3.828	1095.151
	SAPMT	-5.690	-3.150	1.451	1036.909
	NMTT	-5.210	-4.281	3.057	1069.262
	MMTT	-4.873	-3.082	2.868	1109.988
	FTA	-5.110	-3.093	2.821	1008.443
	VTA	-4.882	-2.823	1.338	1392.106
PBE	3-DTAT	-5.163	-1.861	2.296	1085.305
	2-DTAT	-5.268	-1.463	2.222	1042.661
	4-DTAT	-5.076	-1.807	2.181	1084.366
	APMT	-4.653	-1.828	1.466	981.873
	4-MAT	-4.726	-1.591	1.487	1155.123
	AMTT	-4.928	-0.898	0.951	550.397
	SAMTT	-4.781	-2.417	1.696	898.441
	DBAMTT	-4.359	-2.528	3.237	941.410
	TR10(2b)	-5.278	-0.698	1.115	1137.079
	TR8(2a)	-5.283	-0.702	1.111	995.156
	APTT	-5.272	-1.929	1.978	759.888
	3,4-MAT	-4.775	-1.778	1.475	1347.053
	MATD	-5.580	-2.742	3.482	1014.818
	HATD	-5.636	-2.815	3.202	945.223
	DMATD	-5.536	-2.731	3.758	1116.268
	SAPMT	-5.511	-2.946	1.569	1056.254
	NMTT	-5.265	-4.072	3.000	1106.876
	MMTT	-4.701	-2.844	3.186	1138.881
	FTA	-4.934	-2.929	2.808	1016.778
	VTA	-4.726	-2.661	1.278	1406.546
PLYB	3-DTAT	-4.982	-1.688	2.283	1089.403
	2-DTAT	-5.209	-1.251	2.220	1046.466
	4-DTAT	-4.927	-1.615	2.198	1087.683
	APMT	-4.514	-1.664	1.519	987.931
	4-MAT	-4.556	-1.427	1.464	1157.908
	AMTT	-4.772	-0.843	0.950	553.124
	SAMTT	-4.610	-2.278	1.716	902.576
	DBAMTT	-4.170	-2.449	3.238	944.981
	TR10(2b)	-5.153	-0.638	1.141	1143.305
	TR8(2a)	-5.157	-0.644	1.130	1000.197
	APTT	-5.137	-1.795	2.001	762.621
	3,4-MAT	-4.612	-1.612	1.503	1355.068
	MATD	-5.475	-2.566	3.477	1020.544

Continued

HATD	-5.564	-2.651	3.177	953.858
DMATD	-5.414	-2.561	3.764	1125.446
SAPMT	-5.184	-2.869	1.803	1063.977
NMTT	-5.112	-3.982	3.092	1120.989
MMTT	-4.523	-2.684	3.222	1137.946
FTA	-4.780	-2.774	2.895	1020.195
VTA	-4.578	-2.494	1.220	1412.068

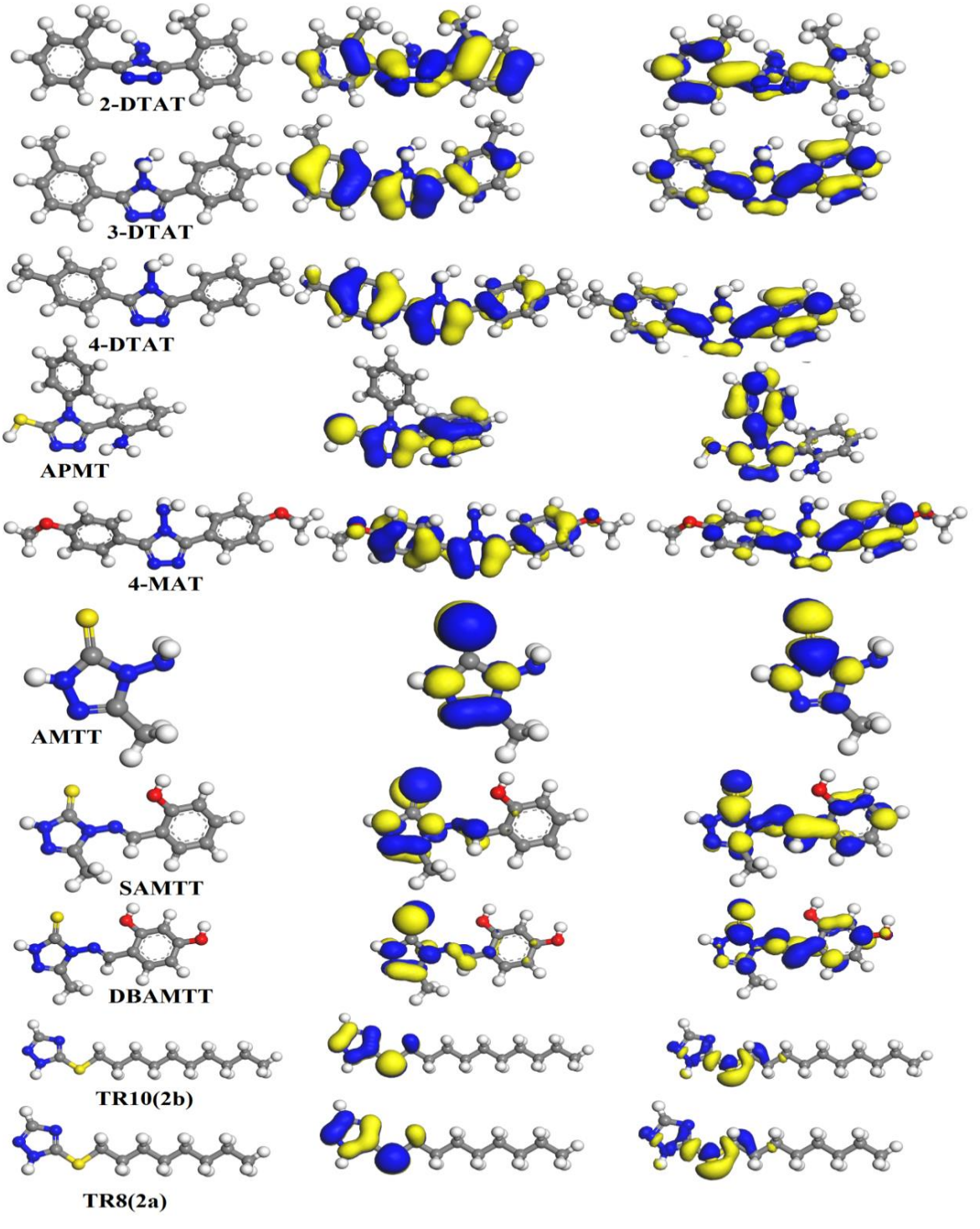

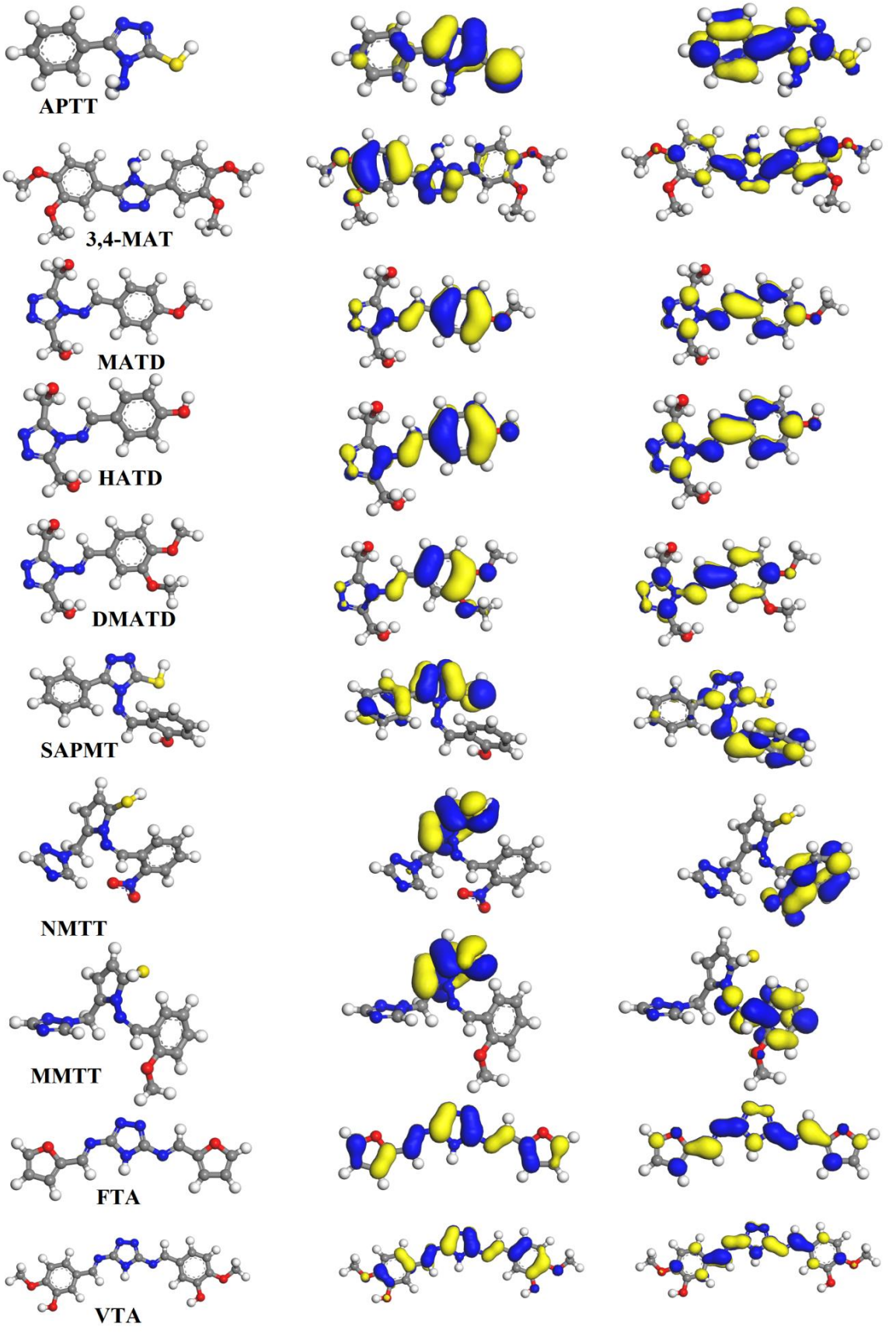

Fig. 2 Optimized Struthers and HOMO, LUMO distributions of Triazole derivatives using AM1.

Table 4. Calculated adsorption energy values for adsorption of triazole derivatives on Fe surface.

	Adsorption energy (Adsorption)	AlogP (Fast Descriptors)
3-DTAT	-154.863	4.856
2-DTAT	-151.126	4.856
4-DTATxsd	-155.334	4.856
APMT	-133.754	3.657
4-MAT	-169.868	3.416
AMTT	-62.4055	0.239
SAMTT	-125.568	2.513
DBAMTT	-127.465	2.229
TR10(2b)	-146.651	4.349
TR8(2a)	-127.475	3.556
APTT	-101.817	2.499
3,4-MAT	-205.359	2.910
MATD	-143.797	2.844
HATD	-132.42	2.812
DMATD	-160.597	2.591
SAPMT	-159.295	4.773
NMTT	-167.276	4.049
MMTT	-164.211	3.843
FTA	-138.314	2.982
VTA	-201.53	3.652

As a result, the adsorption could be physical, and the interactions between the inhibitors and the metal surface could be attributed to π stacking hyperconjugation interactions. However, only total dipole moment values are in line with IE_{exp} in this study using four methods. As shown in Fig. 2 the distributions of HOMO of inhibitor molecules are concentrated mainly around the heteroatoms and aromatic system as well for the studied molecules. Log of the partition coefficient (AlogP) is a molecular descriptor that can be employed on the molecular structure to observe chemical behavior and describes the solubility requirements of a good inhibitor. Generally, adsorption occurs in the surface area of the molecule (SA) and the increase in inhibition efficiency may be due to the SA of the inhibitor molecule.[39-43]

Monte Carlo simulations were carried out on a system containing Fe surface. Fe (110) is a densely packed surface and has the most stabilization, so we choose Fe (110) surface to simulate the adsorption process. Table 4 presents the adsorption energy of all the studied molecules.[44-47]

The QSAR of the studied molecules in Fig. 1 as corrosion inhibitors for mild steel in HCl medium was performed using several methods AM1, PM3, PM6, Perdew-Wang (PWC), Perdew, Burke and Enzerhof (PBE) and Lee-Yang-Parr correlation functional (BLYP). The experimental inhibition efficiency (IE_{exp}) values of the inhibitors were collected from the literature. Furthermore, to make accurate assumptions about productivity, there must be a close correlation between quantum parameters and corrosion inhibitor behavior. However, no straightforward relationship exists between any of these parameters and inhibition efficiencies. As a result, the non-linear model (NLM) that was suggested by Lukovits *et al* to study[43] the interaction between metal surfaces and corrosion inhibitors in corrosive media was derived from and it is based on the Langmuir adsorption isotherm, yielding the following relationship Eq. (1)

$$IE_{calc} = \frac{(Ax_j+B)C_i}{1+(Ax_j+B)C_i} \quad (1)$$

where A and B are constants obtained by regression analysis; xj is a quantum chemical index characteristic for the molecule j; Ci denotes the inhibitor concentration.

$$IE_{calc} = \frac{a\times E_{HOMO}+b\times E_{LUMO}+c\times\mu+d\times SA+e\times\Delta E+f\times E_{ads}+g\times T+h\times C_i+i\times AlogP}{1+a\times E_{HOMO}+b\times E_{LUMO}+c\times\mu+d\times SA+e\times\Delta E+f\times E_{ads}+g\times T+h\times C_i+i\times AlogP} \quad (2)$$

where the constants from a to i are collected from regression analysis and their values are listed in Table 5. The non-linear regression analysis for AM1, PM3, PM6, PWC, PBE, and BLYP was presented in Eq. (2). All the calculations were regressed to Eq. (2) to have the same form with different parameters values (a to i).

The excellent correlation coefficients R^2 and R have been found between IE_{exp} and IE_{calc} where R^2 ranged from 0.857 to 0.967 and R was laid between 0.926 and 0.974. The values of IE_{calc} and its correlation coefficients (R^2 and R) for each method are listed in Table 6 and Table 7. The pattern of the average values of $IE_{calc(Avg)}$ and IE_{exp} of the triazoles derivatives at different concentrations are presented in Fig. 3 and Fig. 5. The correlations between IE_{exp} and $IE_{calc(Avg)}$ of the compounds are presented in Fig. 4. Fig. 6. A very high correlation coefficient was noticed in Fig. 4 and Fig. 6. This means that the experimental and calculated values are highly correlated. According to statistical parameters, the evolved models have a high R^2, indicating that the proposed model is stable and predictive.[38-47]

Table 5. Values of regression constants outputs.

Method	a	b	c	d	e	f	g	h	i
Semiempirical Method									
AM1	2.2644	12.6783	0.8168	0.1573	0.1752	-0.5959	0.6103	3545.6579	-1.4873
PM3	0.6919	6.2289	-0.4041	0.3917	0.0546	-0.4398	0.3504	3828.2454	-0.1116
PM6	2.6333	6.3128	0.2380	0.1245	0.1641	-0.4164	0.8856	2684.3181	0.0324
DFT Method									
PWC	7.9839	-1.5050	-1.8906	0.0054	0.1208	-0.1149	1.2199	6856.4754	-0.2282
BPE	7.6606	-0.8200	-2.2172	-0.1949	-0.0092	-0.1268	1.2310	6593.4842	0.2789
PLYB	8.0616	-0.9266	-2.0135	-0.0721	-0.0258	-0.1169	1.2824	6.2068	0.5319

Table 6. IE_{exp} was obtained using weight loss of triazole compounds and IE_{calc} was obtained by the proposed equations using semiempirical calculation methods.

				IE_{calc}			
	R			0.974	0.956	0.959	0.935
	R^2			0.949	0.914	0.920	0.967
	Compound	Ci	IE_{exp}	AM1	PM3	PM6	IE_{calc}(avg)
1	3-DTAT	5.00E-04	0.921	0.923	0.925	0.928	0.926
2	2-DTAT	5.00E-04	0.883	0.886	0.873	0.890	0.900
3	4-DTAT	5.00E-04	0.957	0.929	0.932	0.937	0.930
4	APMT	9.32E-05	0.834	0.850	0.862	0.867	0.881
5	4-MAT	4.00E-04	0.980	0.955	0.949	0.951	0.944
6	AMTT	7.00E-04	0.730	0.727	0.728	0.729	0.794
7	SAMTT	7.00E-04	0.930	0.935	0.929	0.928	0.930
8	DBAMTT	7.00E-04	0.940	0.926	0.925	0.924	0.925
9	TR10(2b)	1.00E-06	0.820	0.806	0.816	0.808	0.847
10	TR8(2a)	1.00E-06	0.800	0.813	0.801	0.805	0.848
11	APTT	8.00E-04	0.918	0.915	0.912	0.901	0.914
12	3,4-MAT	1.00E-04	0.985	0.966	0.955	0.969	0.954
13	MATD	1.53E-03	0.911	0.923	0.923	0.928	0.926
14	HATD	1.61E-03	0.882	0.895	0.913	0.911	0.910
15	DMATD	1.37E-03	0.938	0.944	0.935	0.952	0.940
16	SAPMT	1.69E-03	0.956	0.948	0.945	0.936	0.936
17	NMTT	1.00E-03	0.896	0.881	0.878	0.882	0.896
18	MMTT	1.00E-03	0.901	0.915	0.923	0.902	0.914
19	FTA	3.00E-04	0.901	0.900	0.912	0.895	0.907
20	VTA	3.00E-04	0.930	0.953	0.957	0.956	0.945

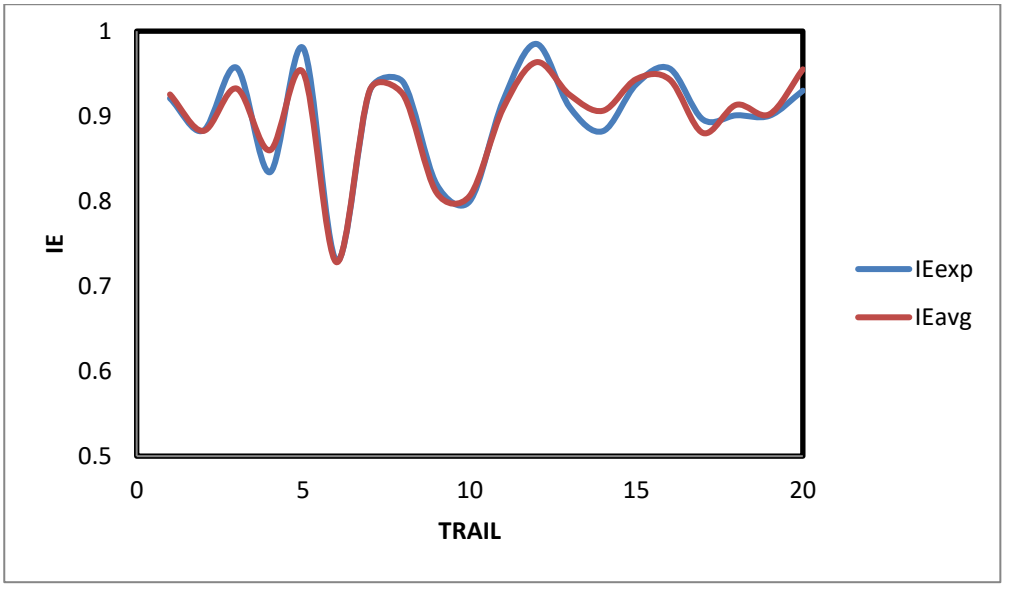

Fig. 3 $IE_{calc(avg)}$ and IE_{exp} at different concentrations of compounds triazole derivatives (semiempirical methods).

Table 7. IE_{exp} was obtained using weight loss of triazole compounds and IE_{calc} was obtained by the proposed equations using DFT calculation methods.

					IE_{calc}			
	R				0.926	0.935	0.959	0.942
	R^2				0.857	0.874	0.920	0.888
	Compound	Ci	*T*	IE_{exp}	PWC	PBE	PLYB	IE_{calc}(avg)
1	3-DTAT	5.00E-04	30	0.921	0.919	0.921	0.925	0.922
2	2-DTAT	5.00E-04	30	0.883	0.912	0.905	0.925	0.914
3	4-DTAT	5.00E-04	30	0.957	0.926	0.927	0.925	0.926
4	APMT	9.32E-05	25	0.834	0.873	0.875	0.925	0.891
5	4-MAT	4.00E-04	30	0.980	0.947	0.946	0.925	0.939
6	AMTT	7.00E-04	27	0.730	0.733	0.733	0.925	0.797
7	SAMTT	7.00E-04	27	0.930	0.922	0.925	0.925	0.924
8	DBAMTT	7.00E-04	27	0.940	0.925	0.929	0.925	0.926
9	TR10(2b)	1.00E-06	30	0.820	0.839	0.837	0.925	0.867
10	TR8(2a)	1.00E-06	30	0.800	0.783	0.783	0.925	0.830
11	APTT	8.00E-04	30	0.918	0.891	0.890	0.925	0.902
12	3,4-MAT	1.00E-04	35	0.985	0.963	0.962	0.925	0.950
13	MATD	1.53E-03	30	0.911	0.935	0.927	0.925	0.929
14	HATD	1.61E-03	30	0.882	0.933	0.925	0.925	0.928
15	DMATD	1.37E-03	30	0.938	0.936	0.928	0.925	0.930
16	SAPMT	1.69E-03	25	0.956	0.934	0.939	0.925	0.933
17	NMTT	1.00E-03	20	0.896	0.889	0.883	0.925	0.899
18	MMTT	1.00E-03	20	0.901	0.892	0.896	0.925	0.904
19	FTA	3.00E-04	28	0.901	0.896	0.905	0.925	0.909
20	VTA	3.00E-04	28	0.930	0.951	0.955	0.925	0.944

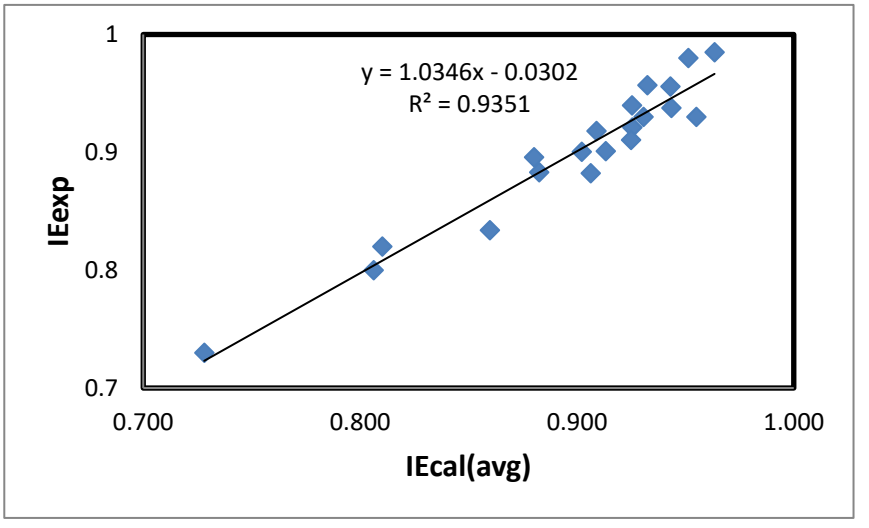

Fig. 4 Correlation between IE_{exp} and $IE_{calc(avg)}$ (semiempirical methods).

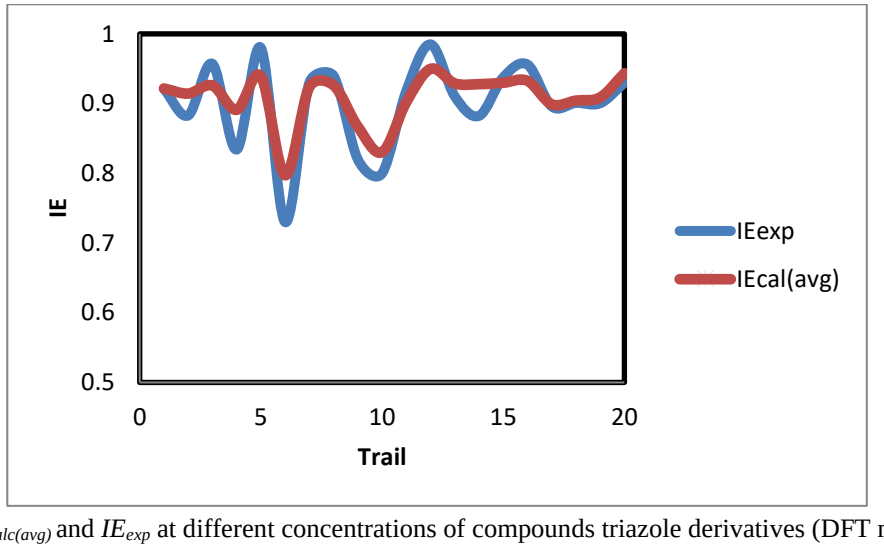

Fig. 5 $IE_{calc(avg)}$ and IE_{exp} at different concentrations of compounds triazole derivatives (DFT methods).

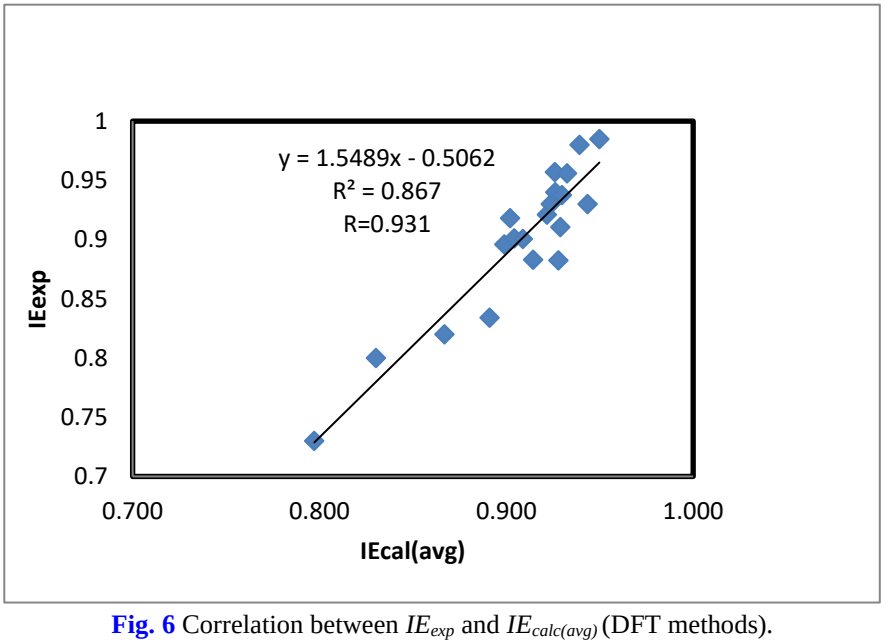

Fig. 6 Correlation between IE_{exp} and $IE_{calc(avg)}$ (DFT methods).

4. Conclusions

The calculated quantum chemical parameters using DFT and semi-empirical methods and Monte Carlo simulation were carried out to corroborate IE_{exp}. The locations containing heteroatoms (S, N, and O), which have high electron density is the most likely bonding sites to the metal surface. (QSAR) studies proved its ability to predict inhibition efficiency. QSAR studies showed that IE_{exp} is well correlated to quantum parameters and E_{ads}. The proposed model has high correlation coefficients, which means that the strength of the model is good and the IE_{calc} is very close to the IE_{exp}.

Supporting information

Not Applicable.

Conflict of interest

There are no conflicts to declare.

References

[1] B. Semire, A. K. Oyebamiji, *New York Science Journal*, 2017, **10**, 11-21, doi: 10.7537/marsnys101217.02.

[2] J. Fang, J. Li, *Journal of Molecular Structure: THEOCHEM*, 2002, **593**, 179-185, doi: 10.1016/s0166-1280(02)00316-0.

[3] T. J. Harvey, F. C. Walsh, A. H. Nahlé, *Journal of Molecular Liquids*, 2018, **266**, 160-175, doi: 10.1016/j.molliq.2018.06.014.

[4] S. A. A. El-Maksoud, *Electrochimica Acta*, 2004, **49**, 4205-4212, doi: 10.1016/j.electacta.2004.04.015.

[5] S. Ouchenane, R.T. Jalgham, S. Rezgoun, H. Saifi, M. Bououdina, *Chemistry Africa*, 2021, 1-13, doi: 10.1007/s42250-021-00239-7.

[6] O. Kozaderov, K. Shikhaliev, C. Prabhakar, A. Tripathi, D. Shevtsov, A. Kruzhilin, E. Komarova, A. Potapov, I. Zartsyn, Y. Kuznetsov, *Applied Sciences*, 2019, **9**, 2821, doi: 10.3390/app9142821.

[7] M. Murmu, S. K. Saha, P. Bhaumick, N. C. Murmu, H. Hirani, P. Banerjee, *Journal of Molecular Liquids*, 2020, **313**, 113508, doi: 10.1016/j.molliq.2020.113508.

[8] N. K. Allam, *Applied Surface Science*, 2007, **253**, 4570-4577, doi: 10.1016/j.apsusc.2006.10.008.

[9] E. S. El Ashry, A. El Nemr, S. Essawy, S. Ragab, *ARKIVOC: Archive for Organic Chemistry*, 2006, 205-220.

[10] F. Bentiss, C. Jama, B. Mernari, H. El Attari, L. El Kadi, M. Lebrini, M. Traisnel, M. Lagrenée, *Corrosion Science*, 2009, **51**, 1628-1635, doi: 10.1016/j.corsci.2009.04.009.

[11] O. Dagdag, A. El Harfi, M. El Gouri, Z. Safi, R. T. T. Jalgham, N. Wazzan, C. Verma, E. E. Ebenso, U. Pramod Kumar, *Heliyon*, 2019, **5**, e01340, doi: 10.1016/j.heliyon.2019.e01340.

[12] O. Dagdag, A. Berisha, Z. Safi, O. Hamed, S. Jodeh, C. Verma, E. E. Ebenso, A. El Harfi, *Journal of Applied Polymer Science*, 2020, **137**, 48402, doi: 10.1002/app.48402.

[13] N. O. Eddy, B. I. Ita, *Journal of molecular modeling*, 2011, **17**, 633-647, doi: 10.1007/s00894-010-0749-x.

[14] M. Lebrini, M. Lagrenée, M. Traisnel, L. Gengembre, H. Vezin, F. Bentiss, *Applied Surface Science*, 2007, **253**, 9267-9276, doi: 10.1016/j.apsusc.2007.05.062.

[15] L. O. Olasunkanmi, B. P. Moloto, I. B. Obot, E. E. Ebenso, *Journal of Molecular Liquids*, 2018, **252**, 62-74, doi: 10.1016/j.molliq.2017.11.169.

[16] B. A. Umar, A. Uzairu, G. A. Shallangwa, *Portugaliae Electrochimica Acta*, 2020, **38**, 313-329, doi: 10.4152/pea.202005313.

[17] S. O. Ajeigbe, N. Basar, Z. Y. Algamal, M. H. Lee, H. Maarof, M. Aziz, *Jurnal Teknologi*, 2017, **79**, doi: 10.11113/jt.v79.9850.

[18] F. Bentiss, M. Lagrenée, B. Elmehdi, B. Mernari, M. Traisnel, H. Vezin, *Corrosion*, 2002, **58**, 399-407, doi: 10.5006/1.3277629.

[19] M. A. Quraishi, R. Sardar, *Corrosion*, 2002, **58**, 748-755, doi: 10.5006/1.3277657.

[20] F. Bentiss, C. Jama, B. Mernari, H. El Attari, L. El Kadi, M. Lebrini, M. Traisnel, M. Lagrenée, *Corrosion Science*, 2009, **51**, 1628-1635, doi: 10.1016/j.corsci.2009.04.009.

[21] M. S. Kumar, S. L. A. Kumar, A. Sreekanth, *Industrial & Engineering Chemistry Research*, 2012, **51**, 5408-5418, doi: 10.1021/ie203022g.

[22] Y. El Aoufir, R. Aslam, F. Lazrak, R. Marzouki, S. Kaya, S. Skal, A. Ghanimi, I. H. Ali, A. Guenbour, H. Lgaz, I. M. Chung, *Journal of Molecular Liquids*, 2020, **303**, 112631, doi: 10.1016/j.molliq.2020.112631.

[23] A. Y. Musa, A. A. H. Kadhum, M. S. Takriff, A. R. Daud, S. K. Kamarudin, N. Muhamad, *Corrosion Engineering, Science and Technology*, 2010, **45**, 163-168, doi: 10.1179/147842208x386359.

[24] M. Tourabi, K. Nohair, A. Nyassi, B. Hammouti, C. Jama, F. Bentiss, *Journal of Materials and Environmental Science*, 2014, **5**, 1133-1143.

[25] M. Prajila, A. Joseph, *Journal of Molecular Liquids*, 2017, **241**, 1-8, doi: 10.1016/j.molliq.2017.05.136.

[26] H. L. Wang, H. B. Fan, J. S. Zheng, *Materials Chemistry and Physics*, 2003, **77**, 655-661, doi: 10.1016/s0254-0584(02)00123-2.

[27] Y. Yan, X. Lin, L. Zhang, H. Zhou, L. Wu, L. Cai, *Research on Chemical Intermediates*, 2017, **43**, 3145-3162, doi: 10.1007/s11164-016-2816-0.

[28] D. Gopi, K. M. Govindaraju, L. Kavitha, *Journal of Applied Electrochemistry*, 2010, **40**, 1349-1356, doi: 10.1007/s10800-010-0092-z.

[29] M. Faisal, A. Saeed, D. Shahzad, N. Abbas, F. Ali Larik, P. Ali Channar, T. Abdul Fattah, D. Muhammad Khan, S. Aaliya Shehzadi, *Corrosion Reviews*, 2018, **36**, 507-545, doi: 10.1515/corrrev-2018-0006.

[30] E. S. H. El Ashry, A. El Nemr, S. A. Essawy, S. Ragab, *Progress in Organic Coatings*, 2008, **61**, 11-20, doi: 10.1016/j.porgcoat.2007.08.009.

[31] F. Bentiss, M. Bouanis, B. Mernari, M. Traisnel, H. Vezin, M. Lagrenée, *Applied Surface Science*, 2007, **253**, 3696-3704, doi: 10.1016/j.apsusc.2006.08.001.

[32] M. Mukaka, *Statistics corner: A guide to appropriate use of correlation coefficient in medical research*, 2012.

[33] F. Bentiss, M. Traisnel, H. Vezin, M. Lagrenée, *Corrosion Science*, 2003, **45**, 371-380, doi: 10.1016/s0010-938x(02)00102-6.

[34] Q. Deng, N. N. Ding, X. L. Wei, L. Cai, X. P. He, Y. T. Long, G. R. Chen, K. Chen, *Corrosion Science*, 2012, **64**, 64-73, doi: 10.1016/j.corsci.2012.07.001.
[35] O. Dagdag, A. El Harfi, Z. Safi, L. Guo, S. Kaya, C. Verma, E. E. Ebenso, N. Wazzan, M. A. Quraishi, A. El Bachiri, M. El Gouri, *Journal of Molecular Liquids*, 2020, **308**, 113020, doi: 10.1016/j.molliq.2020.113020.
[36] A. Y. Musa, R. T. T. Jalgham, A. B. Mohamad, *Corrosion Science*, 2012, **56**, 176-183, doi: 10.1016/j.corsci.2011.12.005.
[37] K. F. Khaled, *Materials Chemistry and Physics*, 2010, **124**, 760-767, doi: 10.1016/j.matchemphys.2010.07.055.
[38] K. F. Khaled, *Electrochimica Acta*, 2010, **55**, 5375-5383, doi: 10.1016/j.electacta.2010.04.079.
[39] A. Y. Musa, A. B. Mohamad, A. A. H. Kadhum, M. S. Takriff, W. Ahmoda, *Journal of Industrial and Engineering Chemistry*, 2012, **18**, 551-555, doi: 10.1016/j.jiec.2011.11.131.
[40] P. M. Álvarez, J. F. García-Araya, F. J. Beltrán, F. J. Masa, F. Medina, *Journal of Colloid and Interface Science*, 2005, **283**, 503-512, doi: 10.1016/j.jcis.2004.09.014.
[41] O. Dagdag, A. Berisha, Z. Safi, S. Dagdag, M. Berrani, S. Jodeh, C. Verma, E. E. Ebenso, N. Wazzan, A. El Harfi, *Journal of Applied Polymer Science*, 2020, **137**, 49003, doi: 10.1002/app.49003.
[42] N. Asadi, M. Ramezanzadeh, G. Bahlakeh, B. Ramezanzadeh, *Journal of the Taiwan Institute of Chemical Engineers*, 2019, **95**, 252-272, doi: 10.1016/j.jtice.2018.07.011.
[43] I. Lukovits, E. Kálmán, G. Pálinkás, *Corrosion*, 1995, **51**, 201-205, doi: 10.5006/1.3294362.
[44] O. Dagdag, Z. Safi, H. Erramli, N. Wazzan, I. B. Obot, E. D. Akpan, C. Verma, E. E. Ebenso, O. Hamed, A. El Harfi, *Journal of Molecular Liquids*, 2019, **287**, 110977, doi: 10.1016/j.molliq.2019.110977.
[45] E. S. H. El Ashry, A. El Nemr, S. A. Esawy, S. Ragab, Corrosion inhibitors, *Electrochimica Acta*, 2006, **51**, 3957-3968, doi: 10.1016/j.electacta.2005.11.010.
[46] J. Cruz, E. Garcia-Ochoa, M. Castro, *Journal of the Electrochemical Society*, 2003, **150**, B26, doi: 10.1149/1.1528197.
[47] N. Khalil, *Electrochimica Acta*, 2003, **48**, 2635-2640, doi: 10.1016/s0013-4686(03)00307-4.

Author information

Ramzi Jalgham *is presently working as an Associate Lecturer in oil and Gas Department, Bani Waleed University, Bani Waleed City, Libya. He got his M. Eng in chemical Engineering in 2012 from Universiti Kebangsaan Malaysia. B.Eng in Chemical Engineering from University of Tripoli, Tripoli, Libya. He Worked in Department of Quality Control and Membrane unit at Pepsi plant in Tripoli city, Libya.2006-2007. He worked in Dept. of Water Desalination Research, Renewable Energies and Water Desalination Research Center, Tripoli, Libya.2007-2009. Experience in training (Trainer) on the Matlab program at the High Pyramid Company 2013-2016. Faculty member at the University of Bani Walid, Department of Oil and Gas Engineering.2016-2021. His research interests are on the use of Heterocyclic Carbon as corrosion inhibitors, DFT studies, processes modeling and optimization, water desalination.*